

The ACS LCID Project XI. On the early time resolution of LG dwarf galaxy SFHs: Comparing the effects of reionization in models with observations*

Antonio Aparicio^{1,2}, Sebastian L. Hidalgo^{1,2}, Evan Skillman³, Santi Cassisi^{4,1}, Lucio Mayer^{5,6}, Julio Navarro⁷, Andrew Cole⁸, Carme Gallart^{1,2}, Matteo Monelli^{1,2}, Daniel Weisz^{9,10,11}, Edouard Bernard¹², Andrew Dolphin¹³ and Peter Stetson¹⁴

ABSTRACT

The analysis of the early star formation history (SFH) of nearby galaxies, obtained from their resolved stellar populations is relevant as a test for cosmological models. However, the early time resolution of observationally derived SFHs is limited by several factors. Thus, direct comparison of observationally derived SFHs with those derived from theoretical models of galaxy formation is potentially biased. Here we investigate and quantify this effect. For this purpose, we analyze the duration of the early star formation activity in a sample of four Local Group dwarf galaxies and test whether they

*Based on observations made with the NASA/ESA Hubble Space Telescope, obtained at the Space Telescope Science Institute, which is operated by the Association of Universities for Research in Astronomy, Inc., under NASA contract NAS 5-26555. These observations are associated with program #10505

¹Instituto de Astrofísica de Canarias. Vía Láctea s/n. E38200 - La Laguna, Tenerife, Canary Islands, Spain; aaj@iac.es, shidalgo@iac.es, carme@iac.es, monelli@iac.es

²Department of Astrophysics, University of La Laguna. Vía Láctea s/n. E38200 - La Laguna, Tenerife, Canary Islands, Spain

³INAF-Osservatorio Astronomico di Collurania, Teramo, Italy; cassisi@oa-teramo.inaf.it

⁴Intitut für Theoretische Physics, University of Zurich, Zürich, Switzerland; lucio@physics.unizh.ch

⁵Department of Physics, Institut für Astronomie, ETH Zürich, Zürich, Switzerland; lucio@phys.ethz.ch

⁶Department of Physics and Astronomy, University of Victoria, BC V8P 5C2, Canada; jfn@uvic.ca

⁷Minnesota Institute for Astrophysics, University of Minnesota, Minneapolis, MN 55455, USA; skillman@astro.umn.edu

⁸School of Physical Sciences, University of Tasmania, Hobart, Tasmania, Australia; andrew.cole@utas.edu.au

⁹Astronomy Department, Box 351580, University of Washington, Seattle, WA 92895, USA; dweisz@uw.edu

¹⁰Department of Astronomy, University of California at Santa Cruz, 1156 High Street, Santa Cruz, CA 95064, USA

¹¹Hubble Fellow

¹²Institute for Astronomy, University of Edinburgh, Royal Observatory, Blackford Hill, Edinburgh EH9 3HJ, UK; ejb@roe.ac.uk

¹³Raytheon, 1151 East Hermans Road, Tucson, AZ 85706, USA; adolphin@raytheon.com

¹⁴Dominion Astrophysical Observatory, Herzberg Institute of Astrophysics, National Research Council, 5071 West Saanich Road, Victoria, British Columbia V9E 2E7, Canada; peter.stetson@nrc-cnrc.gc.ca

are consistent with being true fossils of the pre-reionization era; i.e., if the quenching of their star formation occurred before cosmic reionization by UV photons was completed. Two classical dSph (Cetus and Tucana) and two dTrans (LGS-3 and Phoenix) isolated galaxies with total stellar masses between 1.3×10^6 to $7.2 \times 10^6 M_{\odot}$ have been studied. Accounting for time resolution effects, the SFHs peak as much as 1.25 Gyr earlier than the optimal solutions. Thus, this effect is important for a proper comparison of model and observed SFHs. It is also shown that none of the analyzed galaxies can be considered a true-fossil of the pre-reionization era, although it is possible that the *outer regions* of Cetus and Tucana are consistent with quenching by reionization.

Subject headings: galaxies:dwarf, galaxies:evolution, galaxies:photometry, galaxies:stellar content, galaxies:structure, cosmology: early universe

1. INTRODUCTION

Dwarf galaxies are at the focus of a major cosmological problem affecting the Λ CDM scenario: the number of dark matter subhalos around Milky Way-type galaxies predicted by Λ CDM simulations is much larger than the number of observed satellite dwarf galaxies (Kauffmann, White, & Guiderdoni 1993; Klypin et al. 1999; Moore et al. 1999). Most proposals to overcome this problem stem from the idea that the smallest halos would have formed very few stars or failed to form stars at all, and that gas would have been removed in an early epoch. In this way, the lowest mass sub-halos would be either completely dark, and thus undetectable, or extremely faint. Two main mechanisms are usually invoked as responsible of the smallest sub-halos failing to have an extended star formation history (SFH): heating from cosmic ultraviolet (UV) background radiation arising from the earliest star formation in the universe (Bullock, Kravtsov, & Weinberg 2000) and internal SN feedback (Mac Low & Ferrara 1999) following the first star formation episodes in the host dwarf galaxy. The cosmic UV background raises the entropy of the intergalactic medium around the epoch of reionization, preventing baryons from falling into the smallest sub-halos and it can also heat and evaporate the interstellar medium of larger sub-halos which have managed some star formation. The former would never form stars while the latter would presently show only a very old stellar population (Mac Low & Ferrara 1999; Sawala et al. 2010; Shen et al. 2014; Benítez-Llambay et al. 2015). Recent high resolution simulations of dwarf galaxy formation show that the cosmic UV radiation field can also still suppress star formation, even when it cannot evaporate the gas from the halos, by simply preventing gas from becoming dense enough to form molecular clouds (Shen et al. 2014), verifying a previous proposal by Schaye (2001).

It has also been proposed that ram pressure stripping in the diffuse corona of the host massive galaxy could very rapidly remove the ISM already heated by the cosmic UV even over a large range of dwarf galaxy masses (Mayer et al. 2007). However, such a mechanism would become dominant later, during the main accretion phase of typical Milky Way-sized halo, at $z < 2$, in principle

allowing star formation to extend for at least a couple of Gyr beyond the epoch of reionization.

Although consensus exists on the important role played by the two former mechanisms, less clear is the mass range of the affected sub-halos (e.g., Gnedin 2000; Kravtsov, Gnedin, & Klypin 2004; Shen et al. 2014; Benítez-Llambay et al. 2015). The fact that most or all of the recently discovered ultra-faint dwarfs (UFDs) appear to host only a small population of very old stars, points to them as possible fossils of this process, but some of the classical dSph galaxies may also be affected. Besides heating the gas, UV photons produce the global cosmic reionization. The redshift at which the universe was fully reionized was $z \sim 6$, as obtained from the presence of the Gunn-Peterson trough in quasars (Loeb & Barkana 2001; Becker et al. 2001), although there is increasing evidence that this process was inhomogeneous (Spitler et al. 2012; Becker et al. 2015; Sobacchi & Mesinger 2015). According to models (see e.g., Ricotti & Gnedin 2005; Gnedin & Kravtsov 2006; Bovill & Ricotti 2011a,b), the minimum circular velocity for a dwarf halo to accrete and cool gas in order to produce star formation is in the range of $v_c \sim 20$ to 30 km s^{-1} , which corresponds to a total mass of $\sim 10^8 - 10^9 M_\odot$. However, while most dwarf galaxies in the Local Group show circular velocities below this range and dynamical masses smaller than $\sim 10^8 M_\odot$ (see e.g., McConnachie 2012), many of them have CMDs that have been interpreted as indicating the presence of star formation activity extended well beyond the reionization epoch, even in old dSph galaxies (Grebel & Gallager 2004; Monelli et al. 2010a,b; Hidalgo et al. 2011; Weisz et al. 2014a,b). Two main mechanisms have been proposed to overcome this problem. The first one is that dwarf halos could have been much larger in the past and have lost a significant amount of mass due to tidal harassment (Kazantzidis et al. 2004; Kravtsov et al. 2004). This scenario is further supported by detailed simulations of the tidal interaction between satellites and the host which includes also the baryonic component and ram pressure stripping (Mayer et al. 2007; Mayer 2010). However, counter-arguments exist pointing to dwarf halos being resilient to tidal harassment (Peñarrubia et al. 2008). The second one is that a self-shielding mechanism would be at work, protecting the gas in the central denser regions of the dwarf galaxy, where gas can be optically thick to the impinging radiation field (Susa & Umemura 2004). The first mechanism is robust, since it is a natural consequence of hierarchical accretion as dwarf satellites move on highly eccentric orbits, suffering strong tidal shocks from the host potential. The second mechanism is more subtle, since models neglect a related, competitive effect, namely that the local UV radiation from the primary galaxy or nearby proto-clusters could have been much higher than the mean cosmic ionizing flux at $z > 1$ (Mayer 2010; Iliev et al. 2011).

Models by Bovill & Ricotti (2011a,b) show that Milky Way satellites with total luminosities $L_V > 10^6 L_\odot$ are very unlikely to be true fossils of the reionization epoch, and that they probably are the result of hierarchical build-up from smaller halos extending beyond the reionization epoch. More specifically, Bovill & Ricotti (2011a) conclude that the simulated properties of true fossils, i.e., those which have not undergone any merging events after reionization, agree with those of a subset of the ultra-faint dwarf satellites of Andromeda and the Milky Way. Also, they found that most classical dSph satellites are unlikely true fossils, although they have properties in common with them: diffuse, old stellar populations and no gas. We note that, while it would seem natural

to associate UFDs to reionization fossils, alternative explanations for their origin have recently appeared in the literature in which at least a fraction of them could be remnants of the oldest, most heavily stripped population of galaxy satellites accreting at $z > 2$ onto the Milky Way halo (Tomozeiu et al. 2015).

Bovill & Ricotti (2011b) used the fraction of star formation produced before reionization as a test to distinguish true fossil galaxies from non-fossils, defining the former as those having produced at least 70% of their stars by $z = 6$. This criterion was defined after the analysis of the theoretical simulations and has the advantage of allowing a thorough comparison of models and observations. In turn, Weisz et al. (2014b) have obtained the SFHs of 38 Local Group dwarf galaxies with stellar masses in the range $10^4 < M_\star < 10^9 M_\odot$, finding that only five of them are consistent with forming the bulk of their stars before reionization and that only two out of the 13 predicted true fossils by Bovill & Ricotti (2011b) show a star formation quenched by reionization. However, it should be noted that the results of Weisz et al. (2014b) are affected by limited time resolution at early ages while the predictions by Bovill & Ricotti (2011b) are free of these effects. These effects are expected to significantly modify the SFHs obtained from observational data, as can be seen in the simulations shown by e.g., Hidalgo et al. (2011) or Hidalgo et al. (2013) among others. As a consequence of this, either observational effects should be simulated in theoretical models or they should be taken into consideration when comparing observational results with the theoretical models. The second is the objective of this paper.

In this paper, we discuss how the temporal resolution limitations of a SFH derived from a CMD might be accounted for. In particular, the goal of this paper is to obtain an estimate of the maximum fraction of mass, *consistent with the observations*, which has been converted into stars by $z = 6$ and of the time by which 70% of the baryonic mass has been converted into stars in each galaxy. These values can be directly compared with the predictions of any theoretical model of star formation in dwarf galaxies and we do this comparison, for illustrative purposes, with some of the most recent ones, currently available in the literature. We have used high resolution SFHs obtained for a set of isolated Local Group dwarfs by the LCID collaboration (Hidalgo et al. 2013, and references therein). Our approach opens a new window to the possibility of testing the effects that cosmic ultraviolet (UV) radiation and internal SN feedback have on the early SFH of dwarf galaxies (whether or not combined with self-shielding or other effects). This is an exploratory paper in which we provide details of the method and apply it to a sample of very well studied dwarf galaxies. Environmental effects, such as tides and ram pressure, affect the mappings between present-day and pre-infall mass satellites and between baryon content and star formation. Therefore, we specifically concentrate on a sample of relatively isolated faint dwarfs. The chosen sample is diverse enough to contain both dIrrs, transition dwarfs and dSphs. In future works, the method will be applied to an extended sample including ultra faint dwarfs.

The structure of the paper is as follows. In Section 2 observational data are described. In Section 3, the proposed method is explained and applied to a sample of four Local Group dwarf galaxies. SFHs from Section 3 are compared in Section 4 with a representative set of state-of-the-

art theoretical models of galaxy formation. The results are discussed in Section 5, together with the main conclusions. As with the previous LCID papers, cosmological parameters of $H_0 = 70.5 \text{ km s}^{-1} \text{ Mpc}^{-1}$, $\Omega_m = 0.274$, and a flat Universe with $\Omega_\Lambda = 1 - \Omega_m$ are assumed (Komatsu et al. 2009).

2. DATA SELECTION

For this work, regarding the observational material, we have used the SFHs of the galaxies Cetus (Monelli et al. 2010a), Tucana (Monelli et al. 2010b), LGS-3 (Hidalgo et al. 2011), and Phoenix (Hidalgo et al. 2009), obtained by the LCID collaboration. Data were obtained with the ACS and WFPC2 onboard HST. The SFHs used in this paper were derived using the IAC method, based on the suite of codes IAC-star/IAC-pop/MinnIAC (Aparicio & Gallart 2004; Aparicio & Hidalgo 2009; Hidalgo et al. 2011). For a more detailed analysis, we have divided the three galaxies with larger field coverages, Cetus, Tucana, and LGS-3, into two regions: an inner one, within one scale length from the center, and an outer one located beyond two scale lengths.

The properties of the galaxies are summarized in Table 1. The total mass in stellar objects (M_\star), V luminosity (L_V), velocity dispersion (σ), and metallicity ($[Fe/H]$) are given. L_V , σ , and $[Fe/H]$ are from McConnachie (2012). The M_\star values are calculated scaling L_V with the mass-luminosity relation obtained from the SFH solution of each galaxy. The L_V values range from 0.5×10^6 to $2.6 \times 10^6 L_\odot$, bracketing the limiting value obtained by Bovill & Ricotti (2011a,b) for galaxies likely to be true fossils.

3. IMPROVING TIME RESOLUTION OF THE SFH AT OLD AGES

Robust SFHs are derived from the CMDs of resolved stellar populations, but they are still affected by several sources of uncertainty that limit time resolution. In short, these sources are of three kinds: (1) those affecting data, (2) those linked to physical properties, and (3) those inherent to the methodology used to derive the SFH. Limitations of the first kind are related to photon counting statistics, defective flat-field corrections, or PSF sampling, among others. Sources of the second kind are mainly distance to the object (contributing to blending and crowding), background and foreground contamination, and differential reddening. The term *observational effects* has often been used by our team to refer to these two kinds combined (see e.g., Aparicio & Hidalgo 2009) and we will adopt it here from now on. They result in limiting the photometry depth and completeness, which in turn vary with stellar colors and magnitudes. They are modeled (e.g., with artificial star tests) and accounted for when synthetic populations are computed. Effects of the third kind refer to the robustness of the method and include the accuracy of the stellar evolution libraries from which synthetic populations are simulated as well as the way in which the best solution is reached. Other items closely related to the physics of the problem like the age-metallicity degeneracy

in the CMD are also involved. All these effects combined result in time resolution limitations and age inaccuracies in the final SFH solutions (Aparicio et al. 1997; Aparicio & Hidalgo 2009; Hidalgo et al. 2011).

To derive the SFH from the CMD of a resolved stellar population one makes a reliable simulation of observational effects (1 and 2 above) in the CMD of one or several synthetic stellar populations. These CMDs are in turn compared with the observational CMD to obtain the SFH (see e.g., Aparicio & Hidalgo 2009; Hidalgo et al. 2011, and references therein). Aparicio & Hidalgo (2009) and Hidalgo et al. (2011) made an analysis of the effects of this process on the time resolution. To a good approximation it can be assumed that all together, the effects on the SFH are similar to a temporal shift plus a convolution with a Gaussian function, G_{obs} . **It should be noticed that average ages of older populations tend to be biased to younger values. This is mainly the effect of the time limit imposed by the method, that does not allow ages older than the age of the universe in the solution.**

The function G_{obs} can be obtained according to the following recipe (see Hidalgo et al. 2011). First, a single burst stellar population with no age dispersion (or a very small one) is computed with the age at which G_{obs} is searched. Second, the observational effects obtained for the galaxy in the artificial star tests are simulated. Third, the SFH of this synthetic population is derived. The result can be taken as G_{obs} .

The G_{obs} function can be used to partially remove the observational effects from the SFH derived for a galaxy. To do so, one can proceed parametrically. We do this by: (i) computing a large number of model SFHs of given shape, peak, and duration; (ii) convolving them with G_{obs} , and (iii) selecting those producing results compatible with the observationally derived SFH. The result of this inverse procedure is not the real, free of errors SFH. The problem we are facing is in fact a bias-variance tradeoff one (see e.g., Hastie et al. 2009). Our objective is removing bias, but the intrinsic variance of the problem remains. Nevertheless it provides a better SFH for comparing to the theoretical models of galaxy formation. This is especially true for the oldest ages, where the limitations on temporal resolution are greatest.

Specifically, we proceed as follows for each observed galaxy field. First, we obtain G_{obs} functions for a range of input ages from 5.0 to 13.0 *Gyr* and we select the one whose resulting peak age is closest to the galaxy SFH peak age. Input ages of the selected G_{obs} functions range from 11.0 (inner LGS-3 field), to 13.0 *Gyr* (outer Cetus and Tucana fields). Second, we have computed a large number of SFHs shaped according to Gaussian functions of amplitude y , mean age τ , and standard deviation σ . We will refer to these trial model SFHs simply as *trial models*. Values of τ have been sampled from 6.0 to 13.5 *Gyr* with step of 0.1 *Gyr*. In turn, σ has been sampled from 0.1 to 6 *Gyr* with steps of 0.1 *Gyr* and with the additional criterion that the resulting functions are truncated for age larger than 13.5 *Gyr*. Trial models include a simple but realistic simulation of the metallicity distribution of the real galaxy for the model age. To this, a gaussian metallicity distribution is used. The mean metallicity is the metallicity observationally obtained for the galaxy

at age τ and the sigma is the metallicity dispersion obtained for the galaxy and the same age. Each trial model shape has been computed a total of 201 times, each one with a different value of y . A total of about 10^6 trial models have been computed for each galaxy field.

In the third step, each trial model has been convolved with the selected G_{obs} function. We will refer by *convolved models* to the results of these convolutions. The fourth step has been to select all the convolved models that are compatible with the SFH obtained for the galaxy field within the error intervals of the latter, including its integral. To apply this criterion, only the age interval $13.2 \leq \text{age} \leq 10.0$ Gyr has been considered. The final step has been to average all the compatible convolved models and, in turn, all the trial models originating them.

Figure 1 shows a summary of the models, including the ones selected for the case of the outer field of the Tucana galaxy. General results are given in Figure 2, which shows that, except for the case of Phoenix, the average of the *good* trial models peaks at older ages and is narrower than the convolved models or the observational SFHs. Following this, the averages of the good trial models will be used to make direct comparisons to theoretical models of galaxy formation.

The Gaussian functions used above are clearly a simplified representation of the SFH. It is not expected to reproduce extended SFHs or those in which recursive star formation bursts are going on for an extended period of time. Indeed, Figure 2 shows that intermediate ages for Phoenix are not well reproduced. Nonetheless it can still be a good approximation for old stellar populations which is the purpose of this exercise. To check for the dependence of the solutions with the trial model shape, we have repeated the same experiments using in turn triangular and step functions. In all the cases results are similar and do not significantly change the conclusions of our work.

Since we are interested here in the fraction of stars formed before a given time, it is better to use the cumulative SFH. We define it as $\Psi(t) = \int_T^t \psi(t') dt'$, where $T = 13.5$ is the age assumed for the onset of the star formation and $\psi(t)$ is the star formation rate. Figure 3 shows the observed and the good trial model cumulative SFHs for all the galaxy fields. The latter is the information needed to make a direct comparison with theoretical models of galaxy formation.

4. COMPARISON WITH THEORETICAL MODELS OF GALAXY FORMATION PREDICTIONS

In Figure 4 the average of the good trial models of the galaxies are compared with a few, representative theoretical models of galaxy formation, namely models 2, 7, and 22 by Sawala et al. (2010), model *Doc* by Shen et al. (2014), and two models by Benítez-Llambay et al. (2015) representative of old and old+intermediate age dwarf galaxies. The latter are those given by the authors by the green curves in their figure 5.

Sawala et al. (2010) have presented high-resolution hydrodynamical simulations of the formation and evolution of isolated dwarf galaxies including the most relevant physical effects, namely,

metal-dependent cooling, star formation, feedback from Type II and Ia SNe, UV background radiation, and internal self-shielding. Models 2 and 7 include UV background radiation and internal self-shielding together with SNe feedback. Model 22 includes only SNe feedback, i.e., it is representative of the case that UV background radiation has no effect on the SFH.

Shen et al. (2014) have carried out fully cosmological, very high resolution, Λ CDM simulations of a set of field dwarf galaxies. Model *Doc* corresponds to a virial mass of $M_{vir} = 1.16 \times 10^{10} M_{\odot}$. Finally, Benítez-Llambay et al. (2015) have used the cosmological hydrodynamical simulation of the Local Group carried on as part of the CLUES project. In all the cases, the reader is referred to the source papers for details.

Some relevant properties of the model galaxies are summarized in Table 1. The total mass in stellar objects (M_{\star}), V luminosity (L_V), velocity dispersion (σ), and metallicity ($[Fe/H]$) are given. M_{\star} is provided by Sawala et al. (2010) and Shen et al. (2014), respectively. Regarding L_V , the values given by Shen et al. (2014) are listed for their models. For the Sawala et al. (2010) models, the L_V are obtained with IAC-star using the model SFHs provided by these authors as input. No data are given for the Benítez-Llambay et al. (2015) models, since these authors do not provide them.

Figure 4 shows that the average of the cumulative good trial models of Cetus, Tucana, and LGS-3 lay between models SM2 and SM7 (both including reionization), on the one side, and models SM22 (without reionization) and BL-1 (average of their oldest models), on the other side. Furthermore, the outer parts of Cetus and Tucana show a reasonable correspondence with SM7, indicating that reionization could have played a role in quenching the star formation in those regions. However, according to this figure, the inner regions of both galaxies plus LGS-3 (inner and outer) and Phoenix seem difficult to reconcile with the Sawala et al. (2010) models with reionization. A good correspondence exists between the inner region of LGS-3 and models BL-1 and SM22, while no good match is found for Phoenix with any of the models considered here. Finally, models BL2, Doc, and Bashful are, by far, too young to reproduce any of the observed galaxies and are likely to be more suitable for much younger galaxies, like IC-1613 (see Skillman et al. 2014).

Bovill & Ricotti (2011b) have defined true fossil galaxies as those having formed all or most of their stars before the reionization era, at $z = 6$. They used the cumulative fraction of star formation produced before reionization as a test to distinguish true fossil galaxies from non-fossils, defining the former as those having produced at least 70% of their stars at $z = 6$, which, for the cosmological parameters adopted here (see above), corresponds to approximately 12.8 Gyr ago. Table 2 gives, for each galaxy field and model, the age at which $\Psi(t) = 0.7$ and the value of $\Psi(t)$ for redshift $z = 6$. Columns 2 and 3 list the values corresponding to the observed SFHs. Columns 4 and 5 give those corresponding to the average of the good trial models. Errors have been obtained from the error bands shown in Figure 3.

Two main conclusions can be obtained from Table 2. First, the age for which the cumulative SFH, $\Psi(t)$ reaches 70% is increased by observational effects by ~ 1.25 Gyr on average, while the

value of $\Psi(t)$ at $z = 6$ is increased by a factor of ~ 1.65 , on average, although it can be larger than two in some cases. This shows that working with the average of good trial models is useful if the earliest evolution of dwarf galaxies is sought. Second, taken at face value, none of the four galaxies analyzed here fulfill the criterion by Bovill & Ricotti (2011b) of having $\Psi(t) \geq 0.7$ at $z = 6$, to be considered true fossils from the pre-reionization era, although the outer regions of Cetus and Tucana might marginally qualify, within a 2σ error interval. In addition, Bovill & Ricotti (2011b) also concluded that galaxies with $L_V > 10^6 L_\odot$ are unlikely true fossils, while those with $L_V < 10^6 L_\odot$ remain reasonable candidates to be fossils of the first galaxy generation. However, three out of the four galaxies considered here have $L_V \leq 10^6 L_\odot$ (Tucana, LGS-3, and Phoenix) and are not true-fossils.

5. SUMMARY AND CONCLUSIONS

In summary, we have presented a method to address the limitations of the temporal resolution of the early SFHs of galaxies derived from deep CMD modeling. We have applied the method to the analysis of the duration of the early star formation activity in a sample of Local Group dwarf galaxies with the purpose of testing whether or not they are true fossils of the pre-reionization era. For a study of this kind to be accurate, the affects of limited time resolution need to be accounted for. For testing for fossils, using SFHs directly derived from deep CMD modeling may produce biased results due to limited time resolution. We have shown elsewhere (Hidalgo et al. 2011) that the SFH derived for a synthetic, single age and metallicity stellar population can be simulated by a Gaussian whose sigma depends on age (G_{obs}). The method presented here consists in computing a large number of stellar populations with Gaussian SFHs and metallicity distribution similar to the on obtained for the galaxy for the same age interval (that we call *trial models*; about 10^6 per galaxy in this case) of varying mean, sigma, and amplitude, and selecting all those that, convolved with G_{obs} , produce results compatible with the optimal SFH directly derived from observations. The average of the good trial models is an improved approach to the real SFH of the galaxy at the very earliest times. In general, the ages of the averages of the good trial models are about ~ 1.25 Gyr older than the optimal SFH solutions for the case of predominantly old galaxies.

We have applied our method to four Local Group dwarfs: Cetus, Tucana, LGS-3, and Phoenix and we have compared our results with predictions made by a number of recent cosmological hydrodynamical simulations for the formation and evolution of dwarf galaxies. A relatively sharp exhaustion of the star formation is necessary at an early epoch, close to $z = 6$, to account for the SFH obtained for the outer region of Tucana and Cetus. The inner part of both galaxies, as well as LGS-3 and, more clearly, Phoenix, are compatible with models predicting more extended star formation activity for dwarf galaxies. However, none of the galaxies and fields studied here, except perhaps the outer regions of Cetus and Tucana, fulfill the criterion to be considered as fossil remnants of the pre-reionization era. As a cautionary note, at present, it cannot be excluded that Cetus and Tucana were affected by environmental effects to some extent. Their distances to the

massive spirals of the LG, while placing them outside the virial radius of either today, is still small enough to admit scenarios in which these galaxies are on nearly radial orbits and they may have already had a close pericenter passage with their host Kazantzidis et al. (2011). If they are bound satellites, their relatively large velocity dispersion, $\sigma \sim 15$ km/s (see Table 1), would make them comparable to the brightest dSph satellites such as Fornax, and implies their halos could have been much more massive before tides began to prune them substantially. If this were the case, it would be likely that their halo mass before infall was high enough to place them clearly above the threshold mass for reionization to play a role, strengthening further the conclusion that they cannot be reionization fossils.

The authors thanks the anonymous referee for her/his comments and suggestions, that help to improve the paper clarity. This work has been funded by the Economy and Competitiveness Ministry of the Kingdom of Spain (grants AYA2010-16717 and AYA2013-42781-P) and by the Instituto de Astrofísica de Canarias (grant P3/94).

REFERENCES

- Aparicio, A., & Gallart, C. 2004, *AJ*, 128, 1465
- Aparicio, A., Gallart, C., & Bertelli, G. 1997, *AJ*, 114, 680
- Aparicio, A., & Hidalgo, S. L. 2009, *AJ*, 138, 558
- Becker, R. H., Fan, X., White, R. L., et al. 2001, *AJ*, 122, 2850
- Becker, G. D., Bolton, J. S., Madau, P., et al. 2015, *MNRAS*, 447, 3402
- Benítez-Llambay, A., Navarro, J. F., Abadi, M. G., et al. 2015, *MNRAS*, 450, 4207
- Bovill & Ricotti 2011a, *ApJ*, 741, 17
- Bovill & Ricotti 2011b, *ApJ*, 741, 18
- Bullock, J. S., Kravtsov, A. V., & Weinberg, D. H. 2000, *ApJ*, 539, 517
- Gnedin, N. Y. 2000, *ApJ*, 542, 535
- Gnedin, N. Y., & Kravtsov, A. V. 2006, *ApJ*, 645, 1054
- Grebel, E. K., & Gallagher, J. S. III 2004, *ApJ*, 610, L89
- Hastie, T., Tibshirani, R., Friedman, J. 2009 *The Elements of Statistical Learning*, Springer-Verlag, New York.
- Hidalgo, S. L., Aparicio, A., Martínez-Delgado, D., & Gallart, C. 2009, *ApJ*, 705, 704

- Hidalgo, S. L., Aparicio, A., Skillman, E., et al. 2011, *ApJ*, 730, 14
- Hidalgo, S. L., Monelli, M., Aparicio, A., et al. 2013, *ApJ*, 778, 103
- Iliev, I. T., Moore, B., Gottlöber, S. et al. 2011, *MNRAS*, 413, 2093
- Kauffmann, G., White, S. D. M., & Guiderdoni, B. 1993, *MNRAS*, 264, 201
- Kazantzidis, S., Mayer, L., Mastropietro, C., et al. 2004, *ApJ*, 608, 663
- Kazantzidis, S., Lokas, E. L., Callegari, S., et al. 2011, *ApJ*, 726, 98
- Klypin, A., Kravtsov, A. V., Valenzuela, O., & Prada, F. 1999, *ApJ*, 522, 82
- Komatsu, E., Dunkley, J., Nolta, M. R., et al. 2009, *ApJS*, 180, 330
- Kravtsov, A. V., Gnedin, O. Y., & Klypin, A. A. 2004, *ApJ*, 609, 482
- Loeb, A., & Barkana, R. 2001, *ARA&A*, 39, 19
- Mac Low, M.-M., & Ferrara, A. 1999, *ApJ*, 513, 142
- Mayer, L., Kazantzidis, S., Mastropietro, & C., Wadsley, 2006, *Nature*, 445, 738
- Mayer, L., 2010, *Advances in Astronomy*, art. id. 278434
- McConnachie, A. W. 2012, *AJ*, 144, 4
- Monelli, M., Hidalgo, S. L., Stetson, P. B., et al. 2010a, *ApJ*, 720, 1225
- Monelli, M., Gallart, C., Hidalgo, S. L., et al. 2010b, *ApJ*, 722, 1864
- Moore, B., Ghigna, S., Governato, F., et al. 1999, *ApJ*, 524, L19
- Peñarrubia, J., Navarro, J. F., & McConnachie, A. W. 2008, *ApJ*, 673, 226
- Ricotti, M., & Gnedin, N. Y. 2005, *ApJ*, 629, 259
- Sawala, T., Scannapieco, C., Maio, U., & White, S. 2010, *MNRAS*, 402, 1599
- Schaye, J. 2001, *ApJ*, 562, L95
- Shen, S., Madau, P., Conroy, C., et al. 2014, *ApJ*, 792, 99
- Skillman, E. D., Hidalgo, S. L., Weisz, D. R., et al. 2014, *AJ*, 786, 44
- Sobacchi, E., & Mesinger, A. 2015, *MNRAS*, 453, 1843
- Spitler, L. R., Romanowsky, A. J., Diemand, J., et al. 2012, *MNRAS*, 423, 2177
- Susa, H., & Umemura, M. 2004, *ApJ*, 610, L5

Tomozeiu, M., Mayer, L., & Quinn, T. 2015, arXiv:1506.02140

Weisz, D. R., Dolphin, A. E., Skillman, E. D., et al. 2014a, ApJ, 789, 147

Weisz, D. R., Dolphin, A. E., Skillman, E. D., et al. 2014b, ApJ, 789, 148

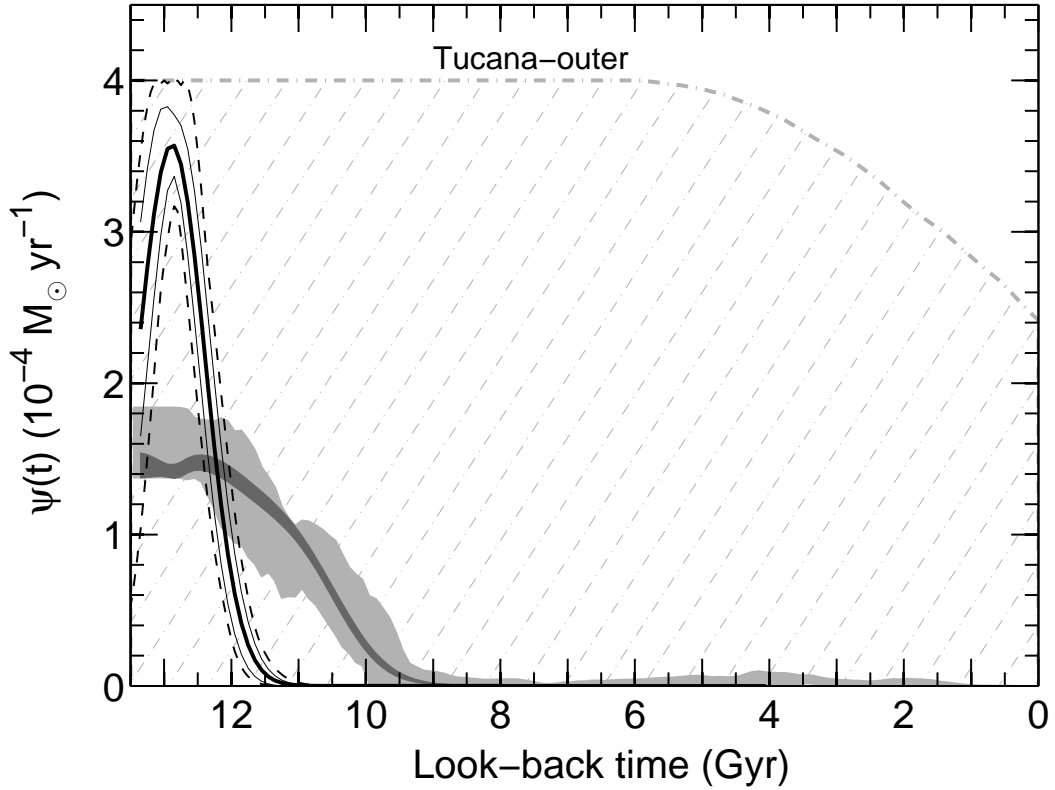


Fig. 1.— Summary of the used models and the good ones selected for the case of Tucana outer field. The grey dashed area shows the envelope of all (about 10^6) the used models. The light grey region shows the SFH of the galaxy including the 1σ error interval estimate. The dark grey region shows the average of convolved-SFHs compatible with empirical results. The wideness shows the 1σ dispersion. Thick, black line shows the average of the good trial models. Thin, black lines show the 1σ dispersion while thin dashed lines are the envelope of all the good trial models.

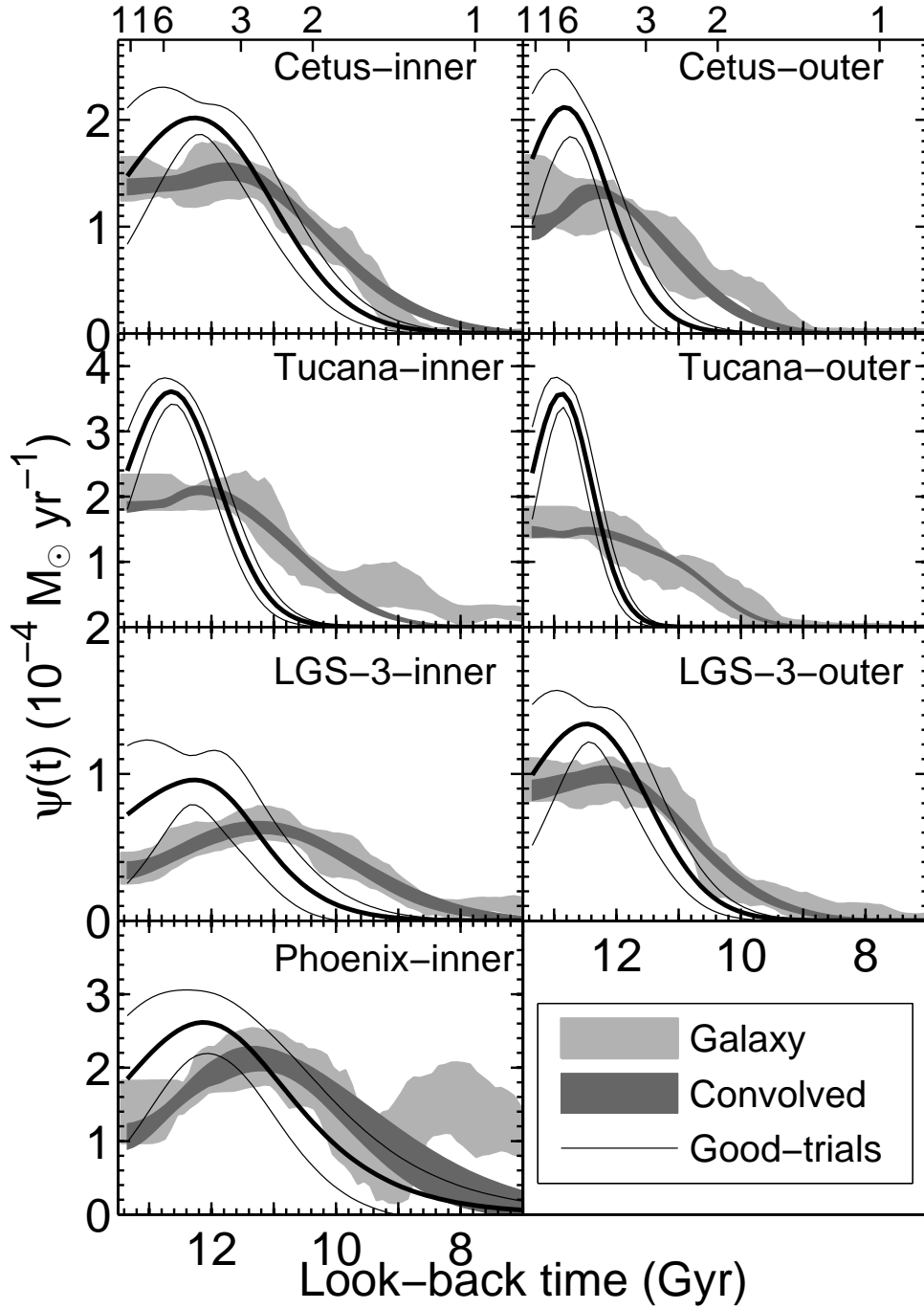


Fig. 2.— SFHs of the galaxy sample compared with good models. Inner and outer regions are shown for Cetus, Tucana and LGS-3 while only the inner region is considered for Phoenix. Light grey regions show the SFHs of galaxies, including the 1σ error interval estimate. Dark grey regions show the average of convolved models compatible with empirical results. The wideness of these regions show the 1σ dispersion. Thick, black lines show the average of the good trial models. Thin, black lines show the 1σ dispersions.

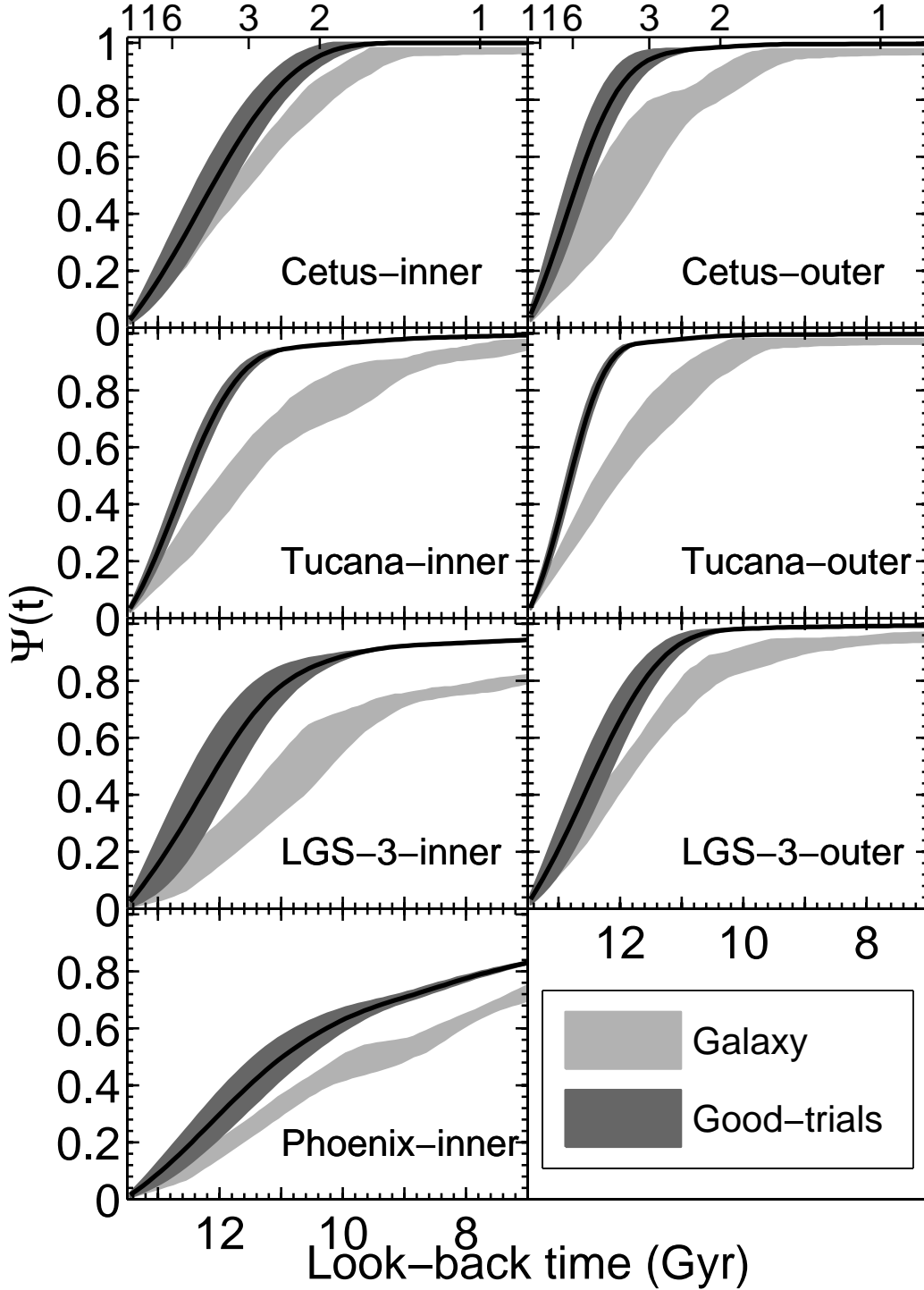


Fig. 3.— Cumulative SFHs for each galaxy field. Light grey areas show the cumulative SFHs derived from observations. Dark grey areas show the same for the average of the good trial models. See main text for details.

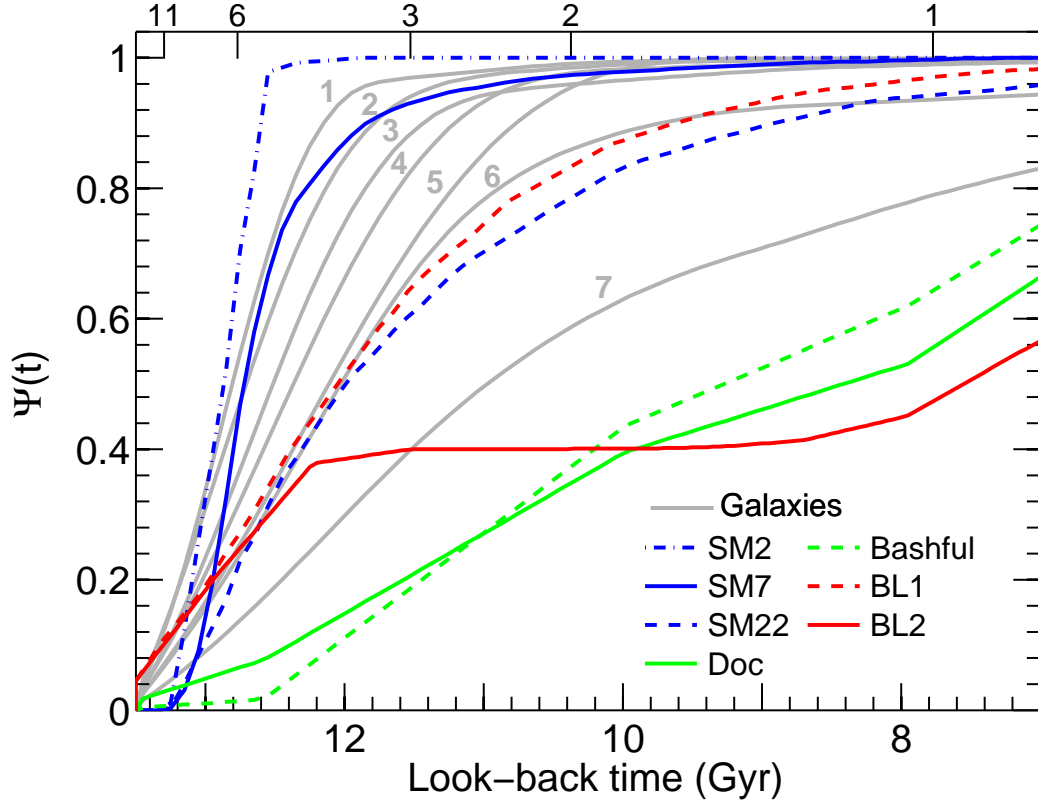


Fig. 4.— Averages of the good trial models in each galaxy field (plotted by thick, black lines in Figure 3) compared with the same for a number of theoretical models of galaxy formation. Numbers in the figure correspond to 1: Tucana-outer, 2: Cetus-outer, 3: Tucana-inner, 4: LGS-3-outer, 5: Cetus-inner, 6: LGS-3-outer, and 7: Phoenix-inner. Regarding to models, SM2, SM7 and SM22 are respectively models 2, 7 and 22 by Sawala et al. (2010). Model "DOC" is by Shen et al. (2014). Models "BL1" and "BL2" are models 1 and 2 by Benítez-Llambay et al. (2015).

Table 1. Summary of data and models

Galaxy/Model	M_* ($10^6 M_\odot$)	L_V ($10^6 L_\odot$)	σ ($km s^{-1}$)	$[Fe/H]$
(1)	(2)	(3)	(4)	(5)
Cetus	7.17	2.58	17.0 ± 2.0	-1.9 ± 0.1
Tucana	1.66	0.54	$15.8^{+4.1}_{-3.1}$	-1.95 ± 0.15
LGS-3	2.08	0.94	$7.9^{+3.2}_{-2.4}$	-2.10 ± 0.22
Phoenix	1.29	0.78	...	-1.37 ± 0.2
S2	0.96	0.43	7.3	-1.76
S7	10.02	4.50	9.1	-1.17
S22	2.58	1.34	7.1	-1.03
Shen13-Doc	34.0	34.04
Shen13-Bashful	115.0	135.52
BL-1
BL-2

Note. — Column 1: data and models identification. Column 2: total stellar mass. Column 3: total V luminosity. Column 4: central velocity dispersion. Column 5: metallicity. For galaxies, L_V , σ and $[Fe/H]$ are from McConnachie 2012; The M_* values are calculated scaling L_V with the mass-luminosity relation obtained from the SFH solution of each galaxy. M_* is provided by Sawala et al. (2010) and Shen et al. (2014), respectively. Regarding L_V , the values given by Benítez-Llambay et al. (2015) are listed for their models. For Sawala et al. (2010) models, the L_V are obtained with IAC-star using the model SFHs provided by these authors as input. No data are given for Benítez-Llambay et al. (2015) models, since these authors do not provide them.

Table 2. Age for $\Psi(t) = 0.7$ and $\psi(t)$ value for $z = 6$

Galaxy field	Age for $\Psi(t)=0.7$ Observational	$\Psi(t)$ at $z = 6$ Observational	Age for $\Psi(t)=0.7$ Good trials	$\Psi(t)$ at $z = 6$ Good trials
Cetus inner	$10.9^{+0.2}_{-0.2}$	$0.22^{+0.03}_{-0.07}$	$11.6^{+0.3}_{-0.4}$	$0.25^{+0.18}_{-0.19}$
Cetus outer	$11.3^{+0.3}_{-0.6}$	$0.28^{+0.09}_{-0.13}$	$12.4^{+0.2}_{-0.3}$	$0.46^{+0.24}_{-0.12}$
Tucana inner	$10.8^{+0.7}_{-0.3}$	$0.21^{+0.05}_{-0.06}$	$12.1^{+0.1}_{-0.1}$	$0.36^{+0.12}_{-0.06}$
Tucana outer	$11.5^{+0.4}_{-0.3}$	$0.29^{+0.03}_{-0.06}$	$12.6^{+0.0}_{-0.1}$	$0.53^{+0.11}_{-0.05}$
LGS-3 inner	$9.4^{+0.3}_{-0.5}$	$0.10^{+0.04}_{-0.06}$	$11.4^{+0.4}_{-0.4}$	$0.23^{+0.25}_{-0.13}$
LGS-3 outer	$11.2^{+0.3}_{-0.2}$	$0.23^{+0.05}_{-0.06}$	$11.9^{+0.3}_{-0.2}$	$0.31^{+0.22}_{-0.11}$
Phoenix inner	$7.3^{+0.3}_{-0.2}$	$0.08^{+0.03}_{-0.03}$	$9.1^{+0.3}_{-0.2}$	$0.13^{+0.05}_{-0.11}$
SM2	12.8	0.98
SM7	12.5	0.67
SM22	11.0	0.31
Shen13-Doc	6.7	0.08
Shen13-Bashful	7.3	0.02
BL-old	11.2	0.34
BL-young	5.8	0.30

Note. — Column 1: Data source: observational inner or outer field for each galaxy or model; observational source: Hidalgo et al. (2013); models sources: Sawala et al. (2010), Shen et al. (2014) and Benítez-Llambay et al. (2015). Column 2: Age at which the cumulative SFH $\Psi(t)$ reaches 70%. Column 3: Value of $\Psi(t)$ corresponding to $z = 6$. Values listed in columns 2 and 3 have been obtained from Figure. 3.